

ICEBERG DRIFT IN THE EASTERN WEDDELL SEA: OBSERVED AND MODELED

Christine Wesche, Thomas Rackow, and Wolfgang Dierking

Alfred Wegener Institute Helmholtz Centre for Polar and Marine Research, Bussestr. 24, 27570 Bremerhaven, Germany,
Email: christine.wesche@awi.de

ABSTRACT

The eastern Weddell Sea region is an alley for drifting icebergs, which calve further east along the coastline of East Antarctica. Our analysis is focused on the region north of the Ekström Ice Shelf. Since at the Ekström Ice Shelf a landing place is used for the supply of the German overwintering station Neumayer III and the South-African station Sanae IV, it is important to monitor the drifting routes taken by the icebergs in this region. We use a series of ENVISAT ASAR WSM data to follow a larger (D18) and a smaller (IB1) iceberg through the eastern Weddell Sea region in 2006. Model simulations are carried out to get more detailed information about the relative influence of different forces on the iceberg drift in this region.

Key words: Icebergs, drift modeling.

1. INTRODUCTION

The eastern Weddell Sea is a region of frequent iceberg sightings. Most icebergs that calve somewhere at the East Antarctic coastline drift along the coast of Dronning Maud Land into the Weddell Sea [3]. The dominant iceberg drift is in a westward direction along the continental slope close to the coastline of Dronning Maud Land [1, 3]. [1] showed that the icebergs are mainly driven by the coastal current (CC) which in turn is driven by the easterly winds [2]. From 52 GPS buoys, which were deployed on small and medium sized icebergs in the Weddell Sea region, mean drift velocities within the CC of 13.7 ± 8.8 km/d were derived [10].

In early 2006, the huge iceberg D18 (named by the National Ice Center - <http://www.natice.noaa.gov/>) drifted along the Ekström Ice Shelf, surrounded by several smaller icebergs. We used a series of 36 ENVISAT ASAR Wide Swath Mode (WSM) images to follow D18 and a smaller iceberg (IB1 - named by the authors) until the end of 2006. In Fig. 1 the first 1.5 months of the drift paths are shown.

In this paper, we present a comparison of observed and modeled iceberg positions. A short overview of the iceberg drift model is given in the following section. It

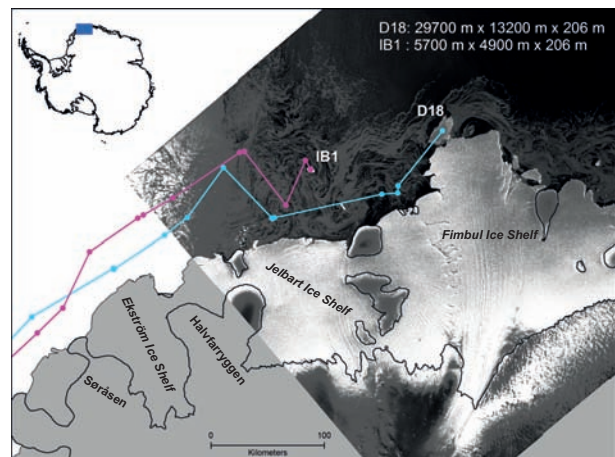


Figure 1. Study region in the eastern Weddell Sea. The two observed icebergs are shown in an ENVISAT ASAR WSM image (image courtesy: ESA). The thin lines show the drift paths of the icebergs. In the upper right corner, the iceberg sizes are listed. The coastline information is taken from [4].

was assumed that wind, ocean currents, and the iceberg draft have different influences on the drift, which was tested by different model settings. The results provide first information about the main driving forces in the eastern Weddell Sea, and they will help to improve the iceberg drift model.

2. ICEBERG DRIFT MODEL

The iceberg drift simulations were performed with a newly implemented iceberg module for FESOM (Finite Elemente Sea-ice Ocean Model [11]). The iceberg model is based on the model formulation presented by [8] with some adjustments, e.g. regarding the numerical discretization and general implementation [9]. The different model components are shown in Fig. 2. As input data observed iceberg starting positions are required. FESOM delivers the draft-integrated ocean velocity (u_o), the sea ice velocity (u_i) and the tilt of the sea surface ($\nabla\eta$). The wind velocity (u_a) is derived from the Coordinated Ocean Research Experiments (CORE.v2 - [7]) forcing data. The

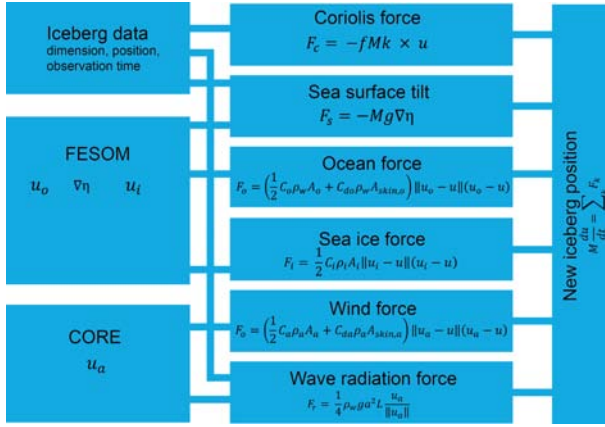


Figure 2. Scheme of the iceberg drift model.

Coriolis force (F_c) is calculated using the mass of the iceberg (M) and the Coriolis parameter $-f = 2\omega \sin\phi$, with $\omega \approx 7.27 * 10^{-5} s^{-1}$ and $\phi = \text{latitude}$. For calculating the ocean and wind force, drag coefficients are used. The form drag coefficient (C_x) describes the drag which acts on the vertical walls of the iceberg and the skin drag coefficient (C_{dx}) the drag which acts on the horizontal walls. The sea ice force depends only on one drag coefficient (C_i). The new position of the iceberg is calculated from the sum of the forces. The model uses a spatial resolution of 10 km close to the coastline and 30 km at larger distances from the shore. A more detailed description of the model is presented by [8] and [9].

3. DRIFT STUDIES

To investigate the relative influence of the winds, ocean currents, sea ice and the iceberg draft on the iceberg drift north of the Ekström Ice Shelf, we released the two icebergs (D18 and IB1) at the acquisition time of the first available SAR image (18.03.2006, 00:33 UTC) into the model and tracked them until 31 December 2006. For our drift studies, we varied the model settings as presented in Table 1. Fixed settings are the Coriolis force, the sea surface tilt, sea ice force and the wave radiation force (Fig. 2, middle). Additionally, the effect of tides and the possibility for icebergs to run aground are implemented. From the SAR images the initial iceberg velocities were estimated and used to initialize the model. The reference run applies the drag coefficients presented in Tab. 1. The parameter *l.freeze* is used to indicate that it is possible that the iceberg drifts with the same velocity as the sea ice. Whether an iceberg is captured in sea ice depends on the ice concentration and its strength. In general, at a concentration of 90 % (9/10) or larger the iceberg is captured if the stress, which the iceberg exerts to the sea ice, is below 13000 Nm^{-1} . If sea ice concentrations are between 15 and 90% the influence of the sea ice on the iceberg drift is calculated using the equation given in Fig. 2. A more detailed description of the general model setting is given in [8] with adjustments as discussed in [9].

To test the influence of wind, ocean, sea ice, and iceberg draft, we switch off or double the respective input parameters (Tab. 1), i.e. we carry out sensitivity studies.

4. RESULTS

The drift paths of the icebergs according to the different model runs are shown in Fig. 3.

In Fig. 3(a and c) the reference run (blue lines and colored dots) is compared to the observed position (Fig. 3, black dots). To ease the reading of the figure, arrows were plotted to show the distances between some of the observed and modeled positions. The reference run shows a problem of the model north of Halvfarryggen (see Fig. 1). The observed positions of D18 and IB1 drift to the north, which is not reproduced by the model results. Another problem occurs north of the Ekström Ice Shelf, where the observed positions are always south of the modeled positions. Looking at the results of the sensitivity studies, which are shown in Fig. 3 (b and d), there are only small differences when varying different input parameters. The most obvious difference was achieved when doubling the wind drag coefficients.

As a measure for the quality of the drift model results, the distances between the observed position (derived from the series of SAR images) and the modeled position is used (Fig. 4). We considered the first 1000 hours of each model run. During the first 900 hours, the distances of D18 and IB1 were in most cases below 100 km (Fig. 4). Afterwards, the distance between the observed and modeled positions of D18 increased, significantly.

5. DISCUSSION

In general, the drift paths of the icebergs were well modeled during all model runs. The drift paths of almost all simulations were very similar. Only the increased wind drag had an obvious influence on the drift of D18 and IB1. The two icebergs were pushed towards the continental shelf. Looking at the observed positions of the icebergs, they followed a contour line of the bathymetry, which leads to the assumption that the bathymetry (and therefore the iceberg draft) had an influence on the iceberg drift. Nevertheless, the doubled iceberg draft did not influence the iceberg drift in our model runs. When doubling the draft of the icebergs, the drag coefficients of the reference run were used.

There was an obvious local northward drift of D18 and IB1 north of the Halvfarryggen (Fig. 3, black dots). Such local changes of drift direction were not resolved by the model. We assume that the main error source of modeling the iceberg drift was the resolution of the forcing data. Local winds and ocean currents, as well as local bathymetric undulations, were not resolved in the data (temporal and spatial).

The distances between the observed and the modeled positions of the icebergs range between 9 km and

Table 1. Model settings.

Parameter	Description	reference	no_si	wind_double	ocean_double	draft_double
C_a^*	wind form drag	0.4	0.4	0.8	0.4	0.4
C_{da}^\dagger	wind skin drag	2.5×10^{-3}	2.5×10^{-3}	5.0×10^{-3}	2.5×10^{-3}	2.5×10^{-3}
C_o^*	ocean form drag	0.85	0.85	0.85	1.7	0.85
C_{do}^\dagger	ocean skin drag	5.0×10^{-3}	5.0×10^{-3}	5.0×10^{-3}	10.0×10^{-3}	5.0×10^{-3}
l_{freeze}	freeze up permission	.true.	.false.	.true.	.true.	.true.
$draft_scale$	iceberg draft	1.0	1.0	1.0	1.0	2.0

* taken from [8]

† taken from [6]

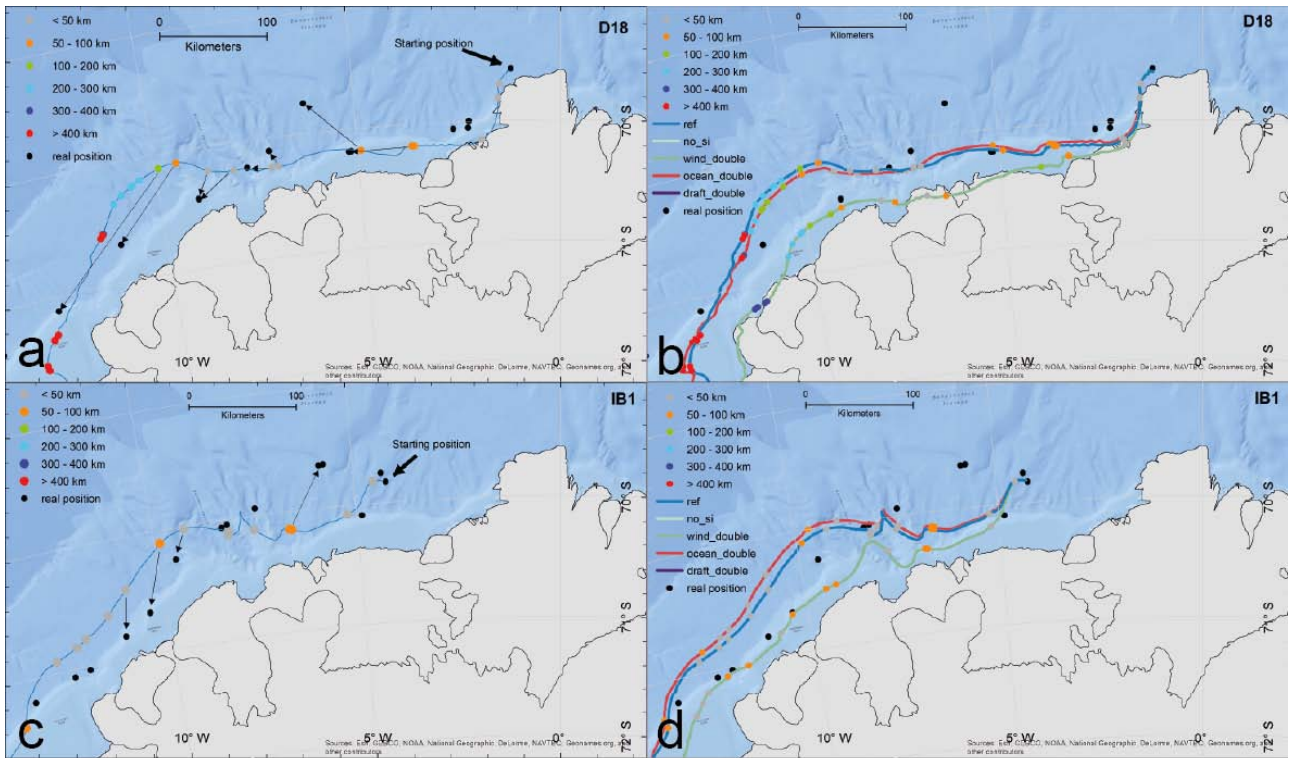


Figure 3. Drift paths of D18 (a and b), IB1 (c and d). The black dots show the observed position of the icebergs and the colored dots present the model position, with a color scale for the distance. In (a) and (c) the reference run is compared to the observed position. The arrows show the true iceberg positions at the same time as the model. In (b) and (d) all model runs are shown together with the observed iceberg positions.

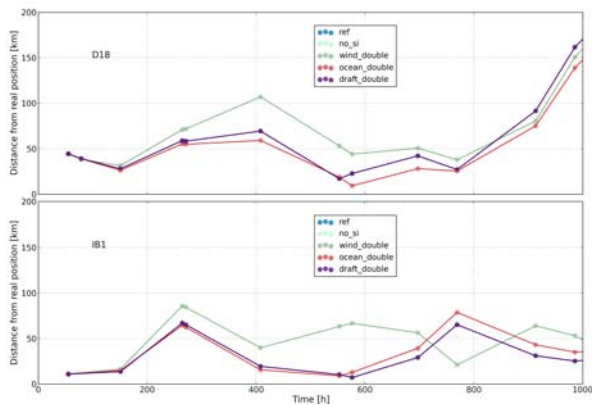


Figure 4. Distances between the observed and modeled iceberg positions.

161 km for D18 and from 7 km to 86 km for IB1 during the first 1000 hours of all model runs. During the first 150 hours, the distances between the observed and the modeled iceberg positions (OM-distances) of all model runs were very similar (Fig. 4). With increasing model time, the OM-distances of the doubled wind drag model-run (*wind_double*) were largest for both icebergs, whereas all other sensitivity runs did not differ significantly from the reference run. The increasing OM-distances calculated for both icebergs with peaks at 407 hours (D18) and 266 hours (IB1), respectively, can be assigned to the local northward drift north of the Halvfarryggen (Fig. 3). Here, the OM-distances were largest for all model settings (Fig. 4). With increasing model time, the variation of OM-distances of the D18 of all model runs became smaller. For IB1, the OM-distances of the *wind_double*-run stayed at about 50 km, decreased to 20 km at 768 hours, where the OM-distances of the other model-runs were large (80 and 60 km). This can be assigned to the region north of the Søråsen (see Fig. 1).

What causes the OM-distances, when the general drift path was modeled well? In general, we obtained lower drift speeds than observed. [5] compared observed sea ice motion obtained from SAR images with FESOM results and found a general underestimation of wind and ocean velocities in the forcing data (e.g. NCEP - <http://www.ncep.noaa.gov/>). The CORE.v2 wind forcing data are based on NCEP reanalyses data, which could be the reason for the lower iceberg drift velocities in our model results.

6. SUMMARY AND OUTLOOK

In this paper, we presented a comparison of observed and modeled iceberg drift in the eastern Weddell Sea region. The drift paths of two icebergs of different sizes (see Fig. 1 - D18 and IB1) were observed with a series of ENVISAT ASAR WSM images starting from 18 March to 26 December 2006. From the first SAR image, we derived the position and the size of the icebergs and started different model runs with different settings (Tab. 1). The

general drift path was modeled well, but comparing the observed iceberg positions to the modeled positions at the time of the SAR image acquisitions, we obtained distances up to 161 km for D18 and 86 km for IB1 for the first 1000 hours of the model runs (Fig. 4). The drift paths of different sensitivity studies look very similar, except for the case when the wind drag was doubled. Here, the icebergs were pushed towards the continental shelf close to the coastline. As the observed iceberg positions follow a contour line of the bathymetry, we assumed that the draft of the iceberg could also have an influence on the iceberg drift. This assumption could not be confirmed when doubling the iceberg draft.

The next steps are detailed investigations of the differences between the observed and modeled iceberg positions.

ACKNOWLEDGMENTS

C. Wesche is funded by the Priority Programme Antarctic Science of the German Research Foundation (DFG SPP 1158 - WE4772/1). The ENVISAT WSM images were provided by ESA for the Cat-1 project C1P.5024.

REFERENCES

- [1] S. Aoki. Seasonal and spatial variations of iceberg drift off Dronning Maud Land, Antarctica, detected by satellite scatterometers. *Journal of Oceanography*, 59(5):629–635, 2003.
- [2] E. Fahrbach, G. Rohardt, and G. Krause. The Antarctic Coastal Current in the southeastern Weddell Sea. *Polar Biology*, 12(2):171–182, 1992.
- [3] R. M. Gladstone, G. R. Bigg, and K. W. Nicholls. Iceberg trajectory modeling and meltwater injection in the Southern Ocean. *Journal of Geophysical Research*, 106(C9):19903–19915, 2001.
- [4] T. Haran, J. Bohlander, T. Scambos, T. Painter, and M. Fahnestock. MODIS mosaic of Antarctica (MOA) image map. Boulder, Colorado, National Snow and Ice Data Center:Digital media, 2005.
- [5] T. Hollands, V. Haid, W. Dierking, R. Timmermann, and L. Ebner. Sea ice motion and open water area at the Ronne Polynia, Antarctica: Synthetic aperture radar observations versus model results. *Journal of Geophysical Research*, 118(4):1940–1954, 2013. doi: 10.1002/jgrc.20158.
- [6] I. Keghouche, L. Bertino, and K. A. Lisaeter. Parameterization of an iceberg drift model in the Barants Sea. *Journal of Atmospheric and Oceanic Technology*, 26(10):2216–2227, 2009. doi: 10.1175/2009JTECHO678.1.
- [7] W. G. Large and S. G. Yeager. The global climatology of an interannually varying air-sea flux data set. *Climate Dynamics*, 33:341–364, 2009. doi: 10.1007/s00382-008-0441-3.

- [8] C. Lichey and H. H. Hellmer. Modeling giant-iceberg drift under the influence of sea ice in the Weddell Sea, Antarctica. *Journal of Glaciology*, 47 (158):452–460, 2001.
- [9] T. Rackow. Modellierung der Eisbergdrift als Erweiterung eines Finite-Elemente-Meereis-Ozean-Modells , diplom thesis, universitt bremen, alfred-wegener-institut fr polar- und meeresforschung. Master's thesis, University of Bremen, 2011.
- [10] M. P. Schodlok, H. H. Hellmer, G. Rohardt, and E. Fahrbach. Weddell Sea iceberg drift: Five years of observations. *Journal of Geophysical Research*, 111(C06018):1–14, 2006. doi: 10.1029/2004JC002661.
- [11] R. Timmermann, S. Danilov, J. Schröter, C. Böning, D. Sidorenko, and K. Rollenhagen. Ocean circulation and sea ice distribution in a finite element global sea ice-ocean model. *Ocean Modelling*, 27 (3-4):114–129, 2009.